Journal of Physics A:
Mathematical and
Theoretical

PAPER • **OPEN ACCESS**

Information-theoretic and operational measures of quantum contextuality

To cite this article: A C Günhan and Z Gedik 2026 *J. Phys. A: Math. Theor.* **59** 195302

Journal of Physics A: Mathematical and Theoretical

PAPER

OPEN ACCESS

RECEIVED
17 December 2025

REVISED
15 April 2026

ACCEPTED FOR PUBLICATION
1 May 2026

PUBLISHED
15 May 2026

Information-theoretic and operational measures of quantum contextuality

A C Günhan[1,*] and Z Gedik[2]

[1] Department of Physics, Mersin University, Çiftlikköy Merkez Yerleşkesi, Yenişehir, Mersin 33150, Türkiye
[2] Faculty of Engineering and Natural Sciences, Sabancı University, Tuzla, Istanbul 34956, Türkiye
[*] Author to whom any correspondence should be addressed.

E-mail: alicangunhan@mersin.edu.tr and gedik@sabanciuniv.edu

Keywords: quantum contextuality, Kochen–Specker theorem, mutual information energy, uncertainty relations, KCBS inequality, Majorana-stellar representation

Supplementary material for this article is available online

Abstract

We propose an information-theoretic framework for quantifying Kochen–Specker contextuality. Two complementary measures are introduced: the mutual information energy, a state-independent quantity inspired by Onicescu's information energy that captures the geometric overlap between joint eigenspaces within a context; and an operational measure based on commutator expectation values that reflects contextual behavior at the level of measurement outcomes. We establish a hierarchy of bounds connecting these measures to the Robertson uncertainty relation, including spectral, purity-corrected, and operator norm estimates. The framework is applied to the Klyachko–Can–Binicioğlu–Shumovsky (KCBS) scenario for spin-1 systems, where all quantities admit closed-form expressions. The Majorana-stellar representation furnishes a common geometric platform on which both the operational measure and the uncertainty products can be analyzed. For spin-1, this representation yields a three-dimensional Euclidean-like visualization of the Hilbert space in which states lying on a plane exhibit maximum uncertainty for the observable along the perpendicular direction; simultaneous optimization across all KCBS contexts singles out a unique state on the symmetry axis. Notably, states achieving the optimal sum of uncertainty products exhibit vanishing operational contextuality, while states with substantial operational contextuality satisfy a nontrivial Robertson bound—the two extremes are realized by distinct quantum states.

1. Introduction: contextuality and measurement in quantum theory

The process and outcome of measurement are fundamentally different in classical and quantum mechanics. In classical (Newtonian) mechanics, the result of a measurement is assumed to exist prior to the act of measurement and remains unaffected by it—only one such measurement can be performed at a time. At the microscopic scale, however, this is no longer the case. Quantum theory allows an arbitrary number of observables to be measured simultaneously on a single system[3], a feature often referred to as *quantum parallelism* [1]. As a result, the state of a quantum system cannot, in general, be prepared in a dispersion-free manner [2], nor can definite outcomes be ascribed to measurements prior to observation [3].

If a system is in an eigenstate of one observable, it is necessarily not an eigenstate of another that does not commute with it—even though both can be measured jointly. Therefore, the outcome of measuring an observable cannot, in general, be independent of the choice of other compatible measurements

[3] Here, 'simultaneous measurement' simply means that the outcomes of different observables can be obtained within the same measurement procedure. Mathematically, a single generalized measurement (POVM, Positive Operator-Valued Measure) may contain very many—indeed, even continuously many–outcomes. In this sense, one quantum measurement can encode information about infinitely many observables, even though not all of them can have sharp values at the same time.

performed concurrently [4–6]. Formally, for observables A, B, and C represented by Hermitian operators $\hat{A}$, $\hat{B}$, and $\hat{C}$ acting on a Hilbert space $\mathcal{H}$ of dimension $d \geqslant 3$, which satisfy

$$\left[\hat{A},\hat{B}\right] = 0, \qquad \left[\hat{B},\hat{C}\right] = 0, \qquad \left[\hat{A},\hat{C}\right] \neq 0, \tag{1}$$

the outcome of a measurement of B depends on whether it is performed alone, together with A, or together with C [7, 8]. In such a situation, the information obtained by measuring (A, B) differs from that obtained by measuring (C, B); hence the measurement of B is *contextual* within the set $\{A, B, C\}$ [9–12]. Accordingly, the question *'How does the information obtained from the measurement of (A,B) differ from that of (C,B)?'* naturally quantifies the *amount of contextuality* associated with B in the context $\{A, B, C\}$. As we illustrate explicitly in section 2, the noncommutativity between the two observables A and C reflects the fact that they implement incompatible refinements of a shared degenerate measurement structure defined by B, which is precisely why the observable B is contextual within the triple $\{A, B, C\}$.

Several quantitative measures of contextuality have been proposed in the literature, most of which are formulated within probabilistic or operational frameworks. Svozil quantified contextuality in terms of the 'frequency of contextual assignments' in a forced tabulation of truth values [13]. Kleinmann *et al* defined it through the *memory cost* of measurement sequences, where the memory corresponds to the number of internal system states reached during sequential measurements, and the cost is its minimum value [14]. Grudka *et al* introduced two measures: the *cost of contextuality*, by analogy with the nonlocality cost [15, 16], and the *relative entropy of contextuality*, analogous to the relative entropy of nonlocality [17], showing that the latter is equivalent to a communication-based measure they also defined [18]. Abramsky *et al* proposed the *contextual fraction*, quantifying how far a quasi-probability representation (allowing non-negative numbers summing to less than unity) can be from a true probability distribution [19]. Kujala and Dzhafarov suggested three alternative measures [20]: two as distances to the *noncontextuality polytope* [21, 22]—in which noncontextual systems are represented on or within the polytope surface—and a third based on quasi-probability distributions allowing negative values whose sum equals unity, where the magnitude of the negative part quantifies the degree of contextuality.

While these approaches differ in formulation, they all share the goal of quantifying the deviation from classical, noncontextual behavior. In the present work, we take an alternative route and formulate contextuality as an information-theoretic property, rooted in the geometric and algebraic relations between measurement subspaces.

The paper is organized as follows. In section 2, we introduce the mutual information energy (MIE) as a state-independent measure of contextuality based on the geometric overlap of joint eigenspaces, and illustrate its definition through explicit projector-level examples, ranging from a minimal abstract setting to a physically relevant spin-1 measurement structure. Section 3 develops the complementary operational measure, which captures contextual behavior at the level of measurement outcomes for a given quantum state, and establishes spectral, purity-corrected, and hybrid bounds that relate this operational quantity to the MIE. In section 4, we connect these bounds to the Robertson uncertainty relation, revealing a hierarchy that ties together the commutator structure, uncertainty products and the geometric MIE quantity. Section 5 illustrates the full framework in the canonical Klyachko–Can–Binicioğlu–Shumovsky (KCBS) scenario for a spin-1 system, where all quantities can be computed in closed form and visualized geometrically. We conclude in section 6 with a summary and outlook.

2. Information-theoretic measure of contextuality

Since the measurement of observables involves obtaining information from a quantum system, and since contextuality concerns how this information depends on the chosen set of compatible measurements, it is natural to treat contextuality as an *information-theoretic property* [23, 24]. A useful scalar quantity in this framework is the *information energy*, originally introduced by Onicescu [25]. For a discrete random variable X taking values $x_1, x_2, \ldots, x_n$ with corresponding probabilities $p_1, p_2, \ldots, p_n$, the information energy is defined as

$$\mathcal{E}(X) = \sum_{i=1}^{n} p_i^2. \tag{2}$$

This quantity serves as an inverse measure of uncertainty: it reaches its maximum for a deterministic (pure) distribution, and its minimum for a uniform one.

Motivated by Onicescu's notion of information energy as a quadratic measure of concentration, we extend this idea to the quantum domain and define the MIE as a *basis-independent, projection-based* quantity that captures the informational overlap between the eigenspaces of different observables.

For observables A, B, C represented by Hermitian operators $\hat{A}$, $\hat{B}$, $\hat{C}$, the MIE is expressed in a projection-based form as

$$E(B;A,C) := \frac{1}{d}\sum_{i,j}\mathrm{Tr}\left[\left(\hat{P}_i^{A,B}\hat{P}_j^{C,B}\right)^2\right], \qquad d=\dim(\mathcal{H})\geqslant 3, \tag{3}$$

where $\hat{P}_i^{A,B}$ and $\hat{P}_j^{C,B}$ are the orthogonal projectors onto the joint eigenspaces of $(\hat{A},\hat{B})$ and $(\hat{C},\hat{B})$, respectively. For $[\hat{A},\hat{B}]=0$, the operators $\hat{A}$ and $\hat{B}$ can be simultaneously diagonalized, and each joint eigenspace is defined as

$$\mathcal{H}_{a,b}^{A,B}=\left\{|\psi\rangle\in\mathcal{H}:\hat{A}|\psi\rangle=a|\psi\rangle,\ \hat{B}|\psi\rangle=b|\psi\rangle\right\},$$

with corresponding projector $\hat{P}_{a,b}^{A,B}$; similarly, $[\hat{C},\hat{B}]=0$ yields

$$\mathcal{H}_{c,b}^{C,B}=\left\{|\psi\rangle\in\mathcal{H}:\hat{C}|\psi\rangle=c|\psi\rangle,\ \hat{B}|\psi\rangle=b|\psi\rangle\right\},$$

with projector $\hat{P}_{c,b}^{C,B}$. Equivalently, if Π_a^A, Π_b^B, and Π_c^C denote the spectral projectors of $\hat{A}$, $\hat{B}$, and $\hat{C}$, then

$$\hat{P}_{a,b}^{A,B}=\Pi_a^A\Pi_b^B\ =\ \Pi_b^B\Pi_a^A, \tag{4}$$

$$\hat{P}_{c,b}^{C,B}=\Pi_c^C\Pi_b^B\ =\ \Pi_b^B\Pi_c^C. \tag{5}$$

The indices i and j in equation (3) enumerate the nonzero joint eigenvalue pairs (a,b) and (c,b). Equation (3) thus quantifies the degree of informational overlap between the subspaces associated with $\hat{A}$ and $\hat{C}$ within each contextual partition defined by $\hat{B}$.

When all three observables mutually commute, they admit a common eigenbasis and hence a common joint spectral decomposition. In that case the two projector families $\{\hat{P}_i^{A,B}\}$ and $\{\hat{P}_j^{C,B}\}$ refine the same partition of $\mathcal{H}$, and after relabeling they may be identified with the same set of joint projectors. Consequently,

$$E(B;A,C)=1, \tag{6}$$

indicating a fully noncontextual situation in which measurement outcomes are jointly definable. More generally, each term $\mathrm{Tr}[(\hat{P}_i^{A,B}\hat{P}_j^{C,B})^2]$ in (3) admits a geometric characterization in terms of the principal angles between the ranges of the two projectors. If $\{|a_k\rangle\}$ and $\{|c_\ell\rangle\}$ denote orthonormal bases for the eigenspaces $\mathcal{H}_i^{A,B}$ and $\mathcal{H}_j^{C,B}$, and σ_μ are the singular values of the overlap matrix $M_{k\ell}=\langle a_k|c_\ell\rangle$, then (see SI, section A)

$$\mathrm{Tr}\left[\left(\hat{P}_i^{A,B}\hat{P}_j^{C,B}\right)^2\right]=\sum_{\mu=1}^{r_{ij}}\sigma_\mu^4, \tag{7}$$

where $r_{ij}=\min(\mathrm{rank}\,\hat{P}_i^{A,B},\mathrm{rank}\,\hat{P}_j^{C,B})$, and $\sigma_\mu=\cos\theta_\mu^{(ij)}$, with $\theta_\mu^{(ij)}$ the principal (canonical) angles between the two subspaces [26]. In the nondegenerate case each projector is rank-1, M reduces to a single scalar $\langle ab_i|cb_j\rangle$, and equation (7) gives

$$\mathrm{Tr}\left[\left(\hat{P}_i^{A,B}\hat{P}_j^{C,B}\right)^2\right]=|\langle ab_i|cb_j\rangle|^4.$$

When, moreover, the eigenbases are mutually unbiased [27–29], i.e. $|\langle ab_i|cb_j\rangle|^2=1/d$ for all i,j, the MIE attains its minimum value,

$$E(B;A,C)=\frac{1}{d}. \tag{8}$$

As a concrete realization, one may take $\hat{B}=\hat{I}$, choose $\hat{A}$ diagonal in the computational basis, and set $\hat{C}=F\hat{A}F^\dagger$ where F is the d-dimensional discrete Fourier transform; the eigenbases of $\hat{A}$ and $\hat{C}$ are then mutually unbiased and each overlap contributes $1/d^2$.

Hence, $E(B;A,C)$ defines a *basis-independent, projection-based measure of contextuality*, robust to degeneracies and directly linked to the geometric overlap of measurement subspaces. In the nondegenerate case where all eigenspaces are one-dimensional, each projector reduces to a rank-1 operator, $\hat{P}_i^{A,B} = |ab_i\rangle\langle ab_i|$, and equation (3) simplifies to

$$E(B;A,C) = \frac{1}{d}\sum_{i,j=1}^{d} |\langle ab_i|cb_j\rangle|^4. \tag{9}$$

This form explicitly shows that $E(B;A,C)$ depends solely on the relative geometry of the eigenspaces of $\hat{A}$ and $\hat{C}$—a purely quantum manifestation of informational compatibility within the context $\{A,B,C\}$.

2.1. Worked examples at the projector level

2.1.1. A minimal abstract example: incompatible refinements of a degenerate observable

To illustrate the projection-based definition of the MIE in its most elementary form we consider a minimal three-dimensional Hilbert space $\mathcal{H} = \mathbb{C}^3$.

Let $\{|e_1\rangle, |e_2\rangle, |e_3\rangle\}$ be an orthonormal basis, and define a degenerate observable

$$\hat{B} = \mathrm{diag}\,(0,1,1)\,, \tag{10}$$

whose eigenspaces consist of a one-dimensional subspace spanned by $|e_1\rangle$ and a two-dimensional degenerate subspace spanned by $\{|e_2\rangle, |e_3\rangle\}$. Such coarse-grained observables are standard in the theory of quantum measurements [1, 30, 31].

We now define two observables $\hat{A}$ and $\hat{C}$ that commute with $\hat{B}$ but correspond to distinct refinements of its degenerate eigenspace.

First refinement. Let $\hat{A}$ be diagonal in the $\{|e_i\rangle\}$ basis, so that the joint-eigenspace projectors of $(\hat{A},\hat{B})$ are

$$\hat{P}_1^{A,B} = |e_1\rangle\langle e_1|, \quad \hat{P}_2^{A,B} = |e_2\rangle\langle e_2|, \quad \hat{P}_3^{A,B} = |e_3\rangle\langle e_3|. \tag{11}$$

Second refinement. Let $\hat{C}$ coincide with $\hat{B}$ on the $|e_1\rangle$ subspace, but resolve the degenerate subspace in the rotated basis

$$|f_\pm\rangle = \frac{1}{\sqrt{2}}\left(|e_2\rangle \pm |e_3\rangle\right). \tag{12}$$

The corresponding joint-eigenspace projectors of $(\hat{C},\hat{B})$ are

$$\hat{P}_1^{C,B} = |e_1\rangle\langle e_1|, \quad \hat{P}_\pm^{C,B} = |f_\pm\rangle\langle f_\pm|. \tag{13}$$

Although both $\hat{A}$ and $\hat{C}$ commute with $\hat{B}$, they define incompatible refinements of the same degenerate eigenspace. We now evaluate the MIE $E(B;A,C)$ explicitly.

Using the definition

$$E(B;A,C) = \frac{1}{d}\sum_{i,j}\mathrm{Tr}\left[\left(\hat{P}_i^{A,B}\,\hat{P}_j^{C,B}\right)^2\right], \qquad d=3, \tag{14}$$

we consider the contributions from the two sectors separately.

Nondegenerate sector. For the one-dimensional eigenspace spanned by $|e_1\rangle$, the projectors coincide:

$$\hat{P}_1^{A,B} = \hat{P}_1^{C,B} = |e_1\rangle\langle e_1|, \tag{15}$$

yielding

$$\mathrm{Tr}\left[\left(\hat{P}_1^{A,B}\hat{P}_1^{C,B}\right)^2\right] = 1. \tag{16}$$

Degenerate sector. For the two-dimensional eigenspace, we compute

$$\hat{P}_2^{A,B}\hat{P}_\pm^{C,B} = |e_2\rangle\langle e_2|f_\pm\rangle\langle f_\pm| = \frac{1}{\sqrt{2}}|e_2\rangle\langle f_\pm|, \tag{17}$$

and similarly for $\hat{P}_3^{A,B}$. Squaring and taking the trace gives

$$\mathrm{Tr}\left[\left(\hat{P}_{2,3}^{A,B}\hat{P}_{\pm}^{C,B}\right)^2\right] = |\langle e_{2,3}|f_{\pm}\rangle|^4 = \frac{1}{4}. \tag{18}$$

There are four such contributions, corresponding to the pairs $(i,j) = (2,\pm)$ and $(3,\pm)$, whose total contribution is $4 \times \frac{1}{4} = 1$.

Result. Collecting all terms, we obtain

$$E(B;A,C) = \frac{1}{3}(1+1) = \frac{2}{3}. \tag{19}$$

This example shows explicitly how the MIE is reduced below unity due to *incompatible refinements* of a shared degenerate observable-eigenspace. In other words, the reduction $E(B;A,C) < 1$ is a direct consequence of the geometry of the joint eigenspaces of $(\hat{A},\hat{B})$ and $(\hat{C},\hat{B})$ (as captured by the joint projectors $\hat{P}_i^{A,B}$ and $\hat{P}_j^{C,B}$, respectively), rather than an artifact of basis choice. In the sense of Kochen–Specker contextuality, this situation corresponds to a contextual observable B: although $[\hat{A},\hat{B}] = 0 = [\hat{C},\hat{B}]$, the incompatibility $[\hat{A},\hat{C}] \neq 0$ implies that the joint-measurement structure of B depends on the compatible context in which it is embedded.

In particular, if $\hat{A}$ and $\hat{C}$ coincide as functions of $\hat{B}$ on each $\hat{B}$-eigenspace, then all three observables commute and equation (3) gives $E(B;A,C) = 1$.

2.1.2. A spin-1 example: degenerate versus nondegenerate measurement structure.
We next illustrate how the projection-based MIE equation (3) operates in a physically relevant spin-1 setting where the contextual partition is altered by the *measurement structure*, in particular by the presence or absence of spectral degeneracy.

Let $\hat{S}_{\mathbf{k}}$ denote the spin-1 operator along a unit direction $\mathbf{k}$, and define the dichotomic observables

$$\hat{A}_{\mathbf{k}} = 2\left(\hat{\mathbf{S}}\cdot\mathbf{k}\right)^2 - \hat{I}, \tag{20}$$

with spectral projectors $\hat{P}_{0_{\mathbf{k}}} = |0_{\mathbf{k}}\rangle\langle 0_{\mathbf{k}}|$ onto the $m_s = 0$ eigenspace [32, 33]. While the operators $\hat{S}_{\mathbf{k}}$ have nondegenerate spectra, the observables $\hat{A}_{\mathbf{k}}$ possess a two-dimensional degenerate eigenspace corresponding to $m_s = \pm 1$.

Let $\mathbf{k}_1$, $\mathbf{k}_2$ and $\mathbf{v}$ be three unit vectors such that $\mathbf{k}_2$ is perpendicular to $\mathbf{k}_1$ and $\mathbf{v}$, and the angle between $\mathbf{k}_1$ and $\mathbf{v}$ is γ. We consider two contexts $\{S_{\mathbf{k}_1}, S^2, S_{\mathbf{v}}\}$ and $\{A_{\mathbf{k}_1}, A_{\mathbf{k}_2}, A_{\mathbf{v}}\}$, and evaluate the mutual information energies using the *joint projectors* of the commuting pairs $(S_{\mathbf{k}_1}, S^2)$, $(S_{\mathbf{v}}, S^2)$ and $(A_{\mathbf{k}_1}, A_{\mathbf{k}_2})$, $(A_{\mathbf{v}}, A_{\mathbf{k}_2})$, respectively.

Evaluating the mutual information energies using the joint projectors of the commuting pairs, one obtains

$$E\left(S^2; S_{\mathbf{k}_1}, S_{\mathbf{v}}\right) = \frac{5 - 2\cos^2\gamma + 9\cos^4\gamma}{12}, \tag{21}$$

and

$$E\left(A_{\mathbf{k}_2}; A_{\mathbf{k}_1}, A_{\mathbf{v}}\right) = \frac{3 - 4\cos^2\gamma + 4\cos^4\gamma}{3}. \tag{22}$$

Although the commuting products in these different contexts can be chosen to share the same eigenbases along the relevant directions, differences in degeneracy structure lead to distinct joint-eigenspace projectors and, consequently, to different values of the MIE.

This comparison demonstrates that the MIE is sensitive to the contextual-measurement partition induced by the choice of contextual observable, as encoded in the geometry of the joint eigenspaces, rather than through eigenvalue spectra alone. A detailed application of these definitions to the full KCBS pentagon, including the evaluation of all contextual triples and the operational measure $D(G,\hat{\rho})$, is presented in section 5.

The definition equation (3) also admits an equivalent characterization in purely algebraic terms. As shown in SI, section B, the MIE satisfies the exact correspondence

$$1 - E(B;A,C) = \frac{1}{2d}\sum_{i,j} \| \left[\hat{P}_i^{A,B}, \hat{P}_j^{C,B}\right] \|_{\mathrm{HS}}^2, \tag{23}$$

where $\|\cdot\|_{\mathrm{HS}}$ denotes the Hilbert–Schmidt norm. This identity shows that the deviation of E from unity is governed by the total noncommutativity of the joint-eigenspace projectors: when all projectors commute, $E=1$ and the context is noncontextual, whereas increasing noncommutativity reduces E, and signals contextual behavior.

Crucially, this commutator formulation provides the link between the basis-independent, geometric notion of contextuality encoded by the MIE and state-dependent, operational quantities. It therefore serves as the starting point for defining an operational measure of contextuality, which we introduce next.

3. Operational contextuality measure

While the MIE $E(B;A,C)$ quantifies the intrinsic, basis-independent geometric overlap associated with a single measurement context, a complementary quantity is required to capture how this contextual structure manifests *operationally*—that is, at the level of measurement outcomes produced by a physical system prepared in a quantum state $\hat{\rho}$. Motivated by the commutator representation equation (23), we therefore introduce a state-dependent operational measure of contextuality defined over a family of contexts

$$G=\{G_\alpha\}_{\alpha=1}^{N}, \qquad G_\alpha=\{A_\alpha,B_\alpha,C_\alpha\}, \tag{24}$$

where each G_α represents a triad of observables whose associated operators satisfy $[\hat{A}_\alpha,\hat{B}_\alpha]=0=[\hat{B}_\alpha,\hat{C}_\alpha]$, defining a distinct measurement context.

3.1. Definition

In analogy with the role of commutators in the Robertson uncertainty relation[4] [34], we quantify the operational signature of contextuality within each context G_α by the magnitude of the commutator expectation value

$$D(G_\alpha,\hat{\rho}) := \left|\mathrm{Tr}\left(\left[\hat{A}_\alpha,\hat{C}_\alpha\right]\hat{\rho}\right)\right|. \tag{25}$$

Summing over all contexts yields the global operational measure

$$D(G,\hat{\rho}) = \sum_{\alpha=1}^{N} D(G_\alpha,\hat{\rho}). \tag{26}$$

This quantity is state dependent and vanishes identically whenever all contexts consist of mutually commuting observables. Conversely, any nonzero contribution reflects an operationally accessible signature of contextuality for the state $\hat{\rho}$.

3.2. Spectral decomposition bound

A general upper bound for $D(G,\hat{\rho})$ follows from the spectral decompositions of the observables. Let

$$\hat{A}_\alpha=\sum_i a_{\alpha i}\hat{P}_{\alpha i}, \qquad \hat{C}_\alpha=\sum_j c_{\alpha j}\hat{Q}_{\alpha j}, \tag{27}$$

where $\hat{P}_{\alpha i}\equiv\hat{P}_i^{A_\alpha,B_\alpha}$ and $\hat{Q}_{\alpha j}\equiv\hat{P}_j^{C_\alpha,B_\alpha}$ are the projectors onto the joint eigenspaces of $(\hat{A}_\alpha,\hat{B}_\alpha)$ and $(\hat{C}_\alpha,\hat{B}_\alpha)$, respectively. By expanding the commutator in terms of these projectors and applying the Cauchy–Schwarz inequality in Hilbert–Schmidt space, one obtains the single-context bound

$$D(G_\alpha,\hat{\rho}) \leqslant \kappa(A_\alpha,C_\alpha)\left[1-E(B_\alpha;A_\alpha,C_\alpha)\right]^{1/2}, \tag{28}$$

where the spectral prefactor is

$$\kappa(A_\alpha,C_\alpha) \equiv \sqrt{2d}\left(\sum_i a_{\alpha i}^2\right)^{1/2}\left(\sum_j c_{\alpha j}^2\right)^{1/2}. \tag{29}$$

[4] We use the Robertson form of the uncertainty relation, which generalizes the familiar Heisenberg bound.

Summing over all contexts yields the global spectral bound

$$D(G,\hat{\rho}) \leqslant \sum_{\alpha=1}^{N} \kappa(A_\alpha, C_\alpha)\,[1 - E(B_\alpha; A_\alpha, C_\alpha)]^{1/2}. \tag{30}$$

The derivation of this bound, which relies on the MIE–commutator correspondence equation (23), is presented in SI, section C. Although completely general, it depends only on the eigenvalues of the observables and the MIE, and therefore may overestimate the true operational contextuality for specific states.

3.3. Purity-corrected bound

The spectral bound (30) can be tightened by retaining the purity of the quantum state. The purity is defined as

$$\beta \equiv \|\hat{\rho}\|_{\mathrm{HS}}^2 = \mathrm{Tr}\left(\hat{\rho}^2\right), \tag{31}$$

and satisfies $1/d \leqslant \beta \leqslant 1$, with $\beta = 1$ for pure states and $\beta = 1/d$ for the maximally mixed state. Incorporating this factor yields the purity-corrected bound

$$D(G_\alpha,\hat{\rho}) \leqslant \sqrt{\beta}\,\kappa(A_\alpha, C_\alpha)\,[1 - E(B_\alpha; A_\alpha, C_\alpha)]^{1/2}. \tag{32}$$

For mixed states with $\beta < 1$, this bound is strictly tighter than (28). The global purity-corrected bound is

$$D(G,\hat{\rho}) \leqslant \sqrt{\beta}\sum_{\alpha=1}^{N} \kappa(A_\alpha, C_\alpha)\,[1 - E(B_\alpha; A_\alpha, C_\alpha)]^{1/2}. \tag{33}$$

3.4. Operator-norm bound

An alternative state-independent bound follows from the duality between the operator norm and the trace norm. For any operator $\hat{X}$ and density matrix $\hat{\rho}$,

$$\left|\mathrm{Tr}\left(\hat{X}\hat{\rho}\right)\right| \leqslant \|\hat{X}\|_{\mathrm{op}}\,\|\hat{\rho}\|_1 = \|\hat{X}\|_{\mathrm{op}}, \tag{34}$$

since $\|\hat{\rho}\|_1 = \mathrm{Tr}(\hat{\rho}) = 1$. Applied to the commutator, this yields

$$D(G_\alpha,\hat{\rho}) \leqslant \|\left[\hat{A}_\alpha, \hat{C}_\alpha\right]\|_{\mathrm{op}}. \tag{35}$$

Since $\|\hat{X}\|_{\mathrm{op}} \leqslant \|\hat{X}\|_{\mathrm{HS}}$ for any operator, the operator-norm bound is at least as tight as a direct application of the Cauchy–Schwarz inequality to $|\mathrm{Tr}([\hat{A},\hat{C}]\,\hat{\rho})|$. However, it does not always dominate the spectral bound (28), which follows a different derivation path through the projector structure and the MIE. The operator-norm bound can be substantially tighter when the observables nearly commute despite having $E(B_\alpha; A_\alpha, C_\alpha) < 1$.

3.5. Hybrid bound

The purity-corrected spectral bound (32) and the operator-norm bound (35) are complementary: the former captures the role of the MIE and state purity, while the latter is state-independent and often tight when the commutator is small. Taking the minimum yields the tightest estimate for a single context:

$$D(G_\alpha,\hat{\rho}) \leqslant \min\left\{\|\left[\hat{A}_\alpha, \hat{C}_\alpha\right]\|_{\mathrm{op}}, \sqrt{\beta}\,\kappa(A_\alpha, C_\alpha)\,[1 - E(B_\alpha; A_\alpha, C_\alpha)]^{1/2}\right\}. \tag{36}$$

Summing over all N contexts, the global hybrid bound reads

$$D(G,\hat{\rho}) \leqslant \sum_{\alpha=1}^{N} \min\left\{\|\left[\hat{A}_\alpha, \hat{C}_\alpha\right]\|_{\mathrm{op}},\ \sqrt{\beta}\,\kappa_\alpha\,[1 - E_\alpha]^{1/2}\right\}, \tag{37}$$

where $\kappa_\alpha \equiv \kappa(A_\alpha, C_\alpha)$ and $E_\alpha \equiv E(B_\alpha; A_\alpha, C_\alpha)$.

The global bound (37) is obtained by summing the single-context bounds and is mathematically valid for any collection of contexts. When contexts share observables—as in the KCBS scenario where each observable participates in two adjacent contexts—the bound remains correct but may be looser than if the contexts were independent. This is because the summation treats each context separately without accounting for correlations introduced by shared observables. The complete derivation of these bounds is given in SI, section C.

3.6. Summary of bounds

The hierarchy of bounds established above can be summarized as follows. The spectral bound,

$$D(G_\alpha,\hat{\rho}) \leqslant \kappa_\alpha \left[1-E_\alpha\right]^{1/2}, \tag{38}$$

is the most general but loosest. The purity-corrected bound,

$$D(G_\alpha,\hat{\rho}) \leqslant \sqrt{\beta}\,\kappa_\alpha \left[1-E_\alpha\right]^{1/2}, \tag{39}$$

improves it for mixed states ($\beta<1$). The operator-norm bound,

$$D(G_\alpha,\hat{\rho}) \leqslant \| \left[\hat{A}_\alpha,\hat{C}_\alpha\right] \|_{\mathrm{op}}, \tag{40}$$

provides an independent, state-independent estimate. Finally, the hybrid bound,

$$D(G_\alpha,\hat{\rho}) \leqslant \min\left\{ \| \left[\hat{A}_\alpha,\hat{C}_\alpha\right] \|_{\mathrm{op}},\ \sqrt{\beta}\,\kappa_\alpha \left[1-E_\alpha\right]^{1/2} \right\}, \tag{41}$$

combines these to yield the tightest available constraint.

Taken together, these bounds clarify how the information-theoretic quantity $E(B;A,C)$ constrains the operational manifestations of contextuality. The geometric overlap encoded in the joint eigenspaces of $(\hat{A},\hat{B})$ and $(\hat{C},\hat{B})$ limits the possible size of the commutator expectation values, with the tightest constraint obtained by incorporating both the algebraic structure of each measurement context and the purity of the quantum state.

4. Contextuality–dependent uncertainty relations

The bounds developed in section 3 constrain the operational contextuality measure $D(G,\hat{\rho})$ in terms of the MIE. In this section we connect these bounds to the Robertson uncertainty relation, revealing a hierarchy that ties together the commutator structure, uncertainty products, and the geometric MIE quantity.

4.1. Robertson lower bound

For a quantum state $\hat{\rho}$, the variance of an observable A_α is

$$(\Delta A_\alpha)^2 = \mathrm{Tr}\left(\hat{A}_\alpha^2\,\hat{\rho}\right) - \left[\mathrm{Tr}\left(\hat{A}_\alpha\,\hat{\rho}\right)\right]^2. \tag{42}$$

The Robertson relation [34] provides a state-dependent lower bound on the product of uncertainties:

$$\frac{1}{2}\left|\mathrm{Tr}\left(\left[\hat{A}_\alpha,\hat{C}_\alpha\right]\hat{\rho}\right)\right| \leqslant (\Delta A_\alpha)(\Delta C_\alpha), \tag{43}$$

where the left-hand side quantifies the operational degree of incompatibility between $\hat{A}_\alpha$ and $\hat{C}_\alpha$ within the context $G_\alpha=\{A_\alpha,B_\alpha,C_\alpha\}$.

Recalling the definition equation (25) of the single-context operational measure, equation (43) can be rewritten as

$$\frac{1}{2}D(G_\alpha,\hat{\rho}) \leqslant (\Delta A_\alpha)(\Delta C_\alpha). \tag{44}$$

Summing over all contexts in $G=\{G_\alpha\}_{\alpha=1}^{N}$ it yields the collective lower bound

$$\frac{1}{2}D(G,\hat{\rho}) \leqslant \sum_{\alpha=1}^{N}(\Delta A_\alpha)(\Delta C_\alpha). \tag{45}$$

4.2. Hierarchy of bounds

Combining the Robertson lower bound (45) with the information-theoretic upper bounds from section 3, we obtain a hierarchy relating the operational measure, the uncertainty products, and the MIE.

From the spectral bound (30), the chain of inequalities reads

$$\frac{1}{2}D(G,\hat{\rho}) \leqslant \sum_{\alpha=1}^{N}(\Delta A_\alpha)(\Delta C_\alpha), \quad D(G,\hat{\rho}) \leqslant \sum_{\alpha=1}^{N}\kappa_\alpha\left[1-E_\alpha\right]^{1/2}, \tag{46}$$

where $\kappa_\alpha \equiv \kappa(A_\alpha, C_\alpha)$ and $E_\alpha \equiv E(B_\alpha; A_\alpha, C_\alpha)$.

Incorporating the purity correction (33) tightens the upper bound for mixed states:

$$\frac{1}{2}D(G,\hat{\rho}) \leqslant \sum_{\alpha=1}^{N}(\Delta A_\alpha)(\Delta C_\alpha), \quad D(G,\hat{\rho}) \leqslant \sqrt{\beta}\sum_{\alpha=1}^{N}\kappa_\alpha\left[1-E_\alpha\right]^{1/2}. \tag{47}$$

Finally, the hybrid bound (37) provides the tightest constraint:

$$\frac{1}{2}D(G,\hat{\rho}) \leqslant \sum_{\alpha=1}^{N}(\Delta A_\alpha)(\Delta C_\alpha), \quad D(G,\hat{\rho}) \leqslant \sum_{\alpha=1}^{N}\min\left\{\|\left[\hat{A}_\alpha,\hat{C}_\alpha\right]\|_{\mathrm{op}},\ \sqrt{\beta}\kappa_\alpha\left[1-E_\alpha\right]^{1/2}\right\}. \tag{48}$$

4.3. Interpretation

This hierarchy reveals the interplay between three distinct quantities:

- The *Robertson lower bound* $\frac{1}{2}D(G,\hat{\rho})$ sets the minimum uncertainty product consistent with the non-commutativity of the observables as experienced by the state $\hat{\rho}$.
- The *uncertainty products* $\sum_\alpha(\Delta A_\alpha)(\Delta C_\alpha)$ quantify the actual spread of measurement outcomes.
- The *information-theoretic upper bounds* constrain how large the operational contextuality can be, given the geometric structure encoded in the MIE.

Although $E(B;A,C)$ does not directly bound the uncertainty products, it limits the operational size of the commutator expectations through $D(G,\hat{\rho})$, thereby determining the contextuality-dependent scale on which the products $(\Delta A_\alpha)(\Delta C_\alpha)$ may vary.

4.4. Transition to explicit examples

At this point it is natural to ask whether these inequalities merely encode an abstract hierarchy, or whether they acquire a concrete operational meaning in a realistic quantum-mechanical system. To demonstrate this explicitly, we now turn to a minimal physical setting that supports Kochen–Specker contextuality: a single spin-1 particle ($d=3$). In this three-dimensional Hilbert space, the KCBS construction provides a canonical family of five dichotomic observables arranged along a pentagonal orthogonality graph. These observables not only exhibit the structural features identified above, but also allow the geometric quantity $E(B;A,C)$, the operational measure $D(G,\hat{\rho})$ and the uncertainty products $(\Delta A)(\Delta C)$ to be computed in closed form and visualized geometrically via the Majorana-stellar representation. Thus, the KCBS scenario serves as an ideal testbed for the full framework developed in the preceding sections.

5. Application to the KCBS scenario

Three-level quantum systems provide the minimal Hilbert-space dimension required for the manifestation of Kochen–Specker contextuality [2, 7–9]. In this section we apply the framework developed above to the KCBS scenario [32], where all quantities admit closed-form expressions, and can be visualized geometrically through the Majorana-stellar representation.

5.1. Spin-1 observables and pentagonal contexts

For a spin-1 particle, the observable $\hat{S}_{\mathbf{k}} = \hat{\mathbf{S}}\cdot\mathbf{k}$ represents the spin component along a unit vector $\mathbf{k}$, with eigenvalues $m_s \in \{-1,0,+1\}$. Following Klyachko *et al* [32], one constructs the dichotomic observable

$$\hat{A}_{\mathbf{k}} = 2\hat{S}_{\mathbf{k}}^2 - \hat{I} = \hat{I} - 2|0_{\mathbf{k}}\rangle\langle 0_{\mathbf{k}}|, \tag{49}$$

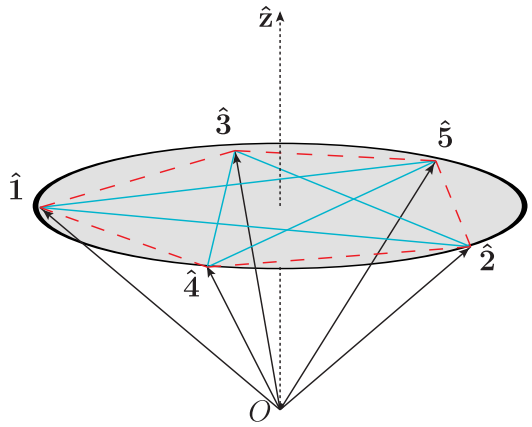

(a) KCBS configuration of five observables forming five overlapping contexts. The five directions $\hat{\mathbf{1}}, \hat{\mathbf{2}}, \hat{\mathbf{3}}, \hat{\mathbf{4}}, \hat{\mathbf{5}}$ lie on a common latitude with equal azimuthal spacing and satisfy the sequential orthogonality convention $\hat{\mathbf{1}} \perp \hat{\mathbf{2}} \perp \hat{\mathbf{3}} \perp \hat{\mathbf{4}} \perp \hat{\mathbf{5}} \perp \hat{\mathbf{1}}$. Each adjacent triplet $\{\hat{A}_{\mathbf{k}}, \hat{A}_{\mathbf{k+1}}, \hat{A}_{\mathbf{k+2}}\}$ defines a context in the KCBS set, and $\hat{A}_{\mathbf{k+5}} = \hat{A}_{\mathbf{k}}$.

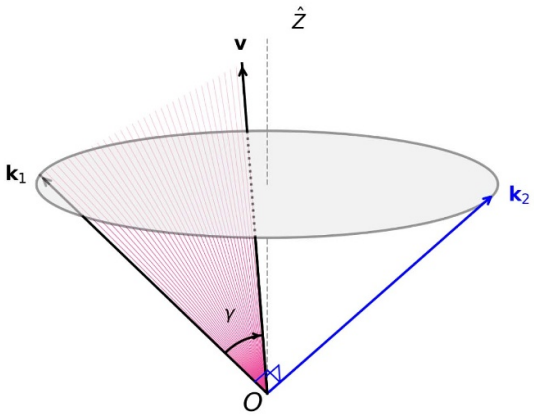

(b) Orientation of a direction $\mathbf{k}_2$ perpendicular to the plane spanned by vectors $\mathbf{k}_1$ and $\mathbf{v}$. For $\gamma = \arccos\frac{\sqrt{5}-1}{2}$, direction $\mathbf{v}$ coincides with $\hat{\mathbf{3}}-$axis shown on the left panel, and the set $\{\hat{A}_{\mathbf{1}}, \hat{A}_{\mathbf{2}}, \hat{A}_{\mathbf{3}}\}$ becomes one of the five KCBS contexts.

Figure 1. KCBS configuration and local orthogonal triad.

which takes eigenvalues $\{+1,+1,-1\}$ with the -1 eigenspace spanned by the $m_s = 0$ state $|0_{\mathbf{k}}\rangle$ along direction $\mathbf{k}$.

The KCBS construction employs five directions $\hat{\mathbf{1}},\ldots,\hat{\mathbf{5}}$ arranged symmetrically about the z-axis, satisfying the cyclic orthogonality condition

$$\mathbf{k} \perp \mathbf{k}+\mathbf{1}, \qquad (\mathrm{mod}\ 5). \tag{50}$$

Geometrically, these five unit vectors lie on a cone of fixed polar angle

$$\theta_{\mathrm{KCBS}} = \arcsin\left(\frac{1}{\sqrt{2}\cos(\pi/10)}\right) \approx 48.03^{\circ},$$

with azimuthal angles

$$\varphi_\alpha = (\alpha-1)\frac{6\pi}{5}, \qquad \alpha \pmod 5,$$

as shown in figure 1(a). Together, this parametrization realizes the cyclic orthogonality in (50), and fixes the geometry of the KCBS pentagon. The angle γ between non-adjacent directions $\mathbf{k}$ and $\mathbf{k}+\mathbf{2}$ is then determined purely by this pentagonal symmetry to be

$$\cos\gamma = \frac{\sqrt{5}-1}{2} \approx 0.618, \qquad \gamma \approx 51.83^{\circ}. \tag{51}$$

This configuration defines five overlapping contexts

$$G_\alpha = \{A_{\alpha-1}, A_\alpha, A_{\alpha+1}\}, \qquad \alpha \pmod 5, \tag{52}$$

where within each context the central observable A_α commutes with both neighbors while the outer pair $\{A_{\alpha-1}, A_{\alpha+1}\}$ do not commute (see figure 1(a)).

5.2. Explicit evaluation of the contextuality measures

An explicit illustration of how the MIE responds to changes of measurement structure and spectral degeneracy was given in section 2. We now specialize this analysis to the KCBS scenario and evaluate the MIE for each contextual triple G_α using the fixed pentagonal geometry.

For each KCBS context G_α, γ is given in equation (51), and the MIE evaluates to

$$E(A_\alpha; A_{\alpha-1}, A_{\alpha+1}) = \frac{3 - 4\cos^2\gamma + 4\cos^4\gamma}{3} \approx 0.685. \tag{53}$$

This result follows directly from equation (3) once the KCBS geometry is fixed. The deviation from unity, $1 - E \approx 0.315$, quantifies the intrinsic contextuality of each KCBS context, and is uniform across all five contexts by virtue of the pentagonal symmetry. Note that $E = 1$ when $\cos\gamma = 0$ or ± 1, corresponding to orthogonal or parallel directions; in these limits the outer observables in the set (52) commute and the context becomes noncontextual, as expected.

The spectral prefactor equation (29) for dichotomic observables with eigenvalues $\{+1, +1, -1\}$ is

$$\kappa(A_{\alpha-1}, A_{\alpha+1}) = \sqrt{2d}\left(\sum_i a_i^2\right)^{1/2}\left(\sum_j {c_j}^2\right)^{1/2} = \sqrt{6} \times 3 \approx 7.35, \tag{54}$$

where $d = 3$ and $\sum_i a_i^2 = \sum_j c_j^2 = 1 + 1 + 1 = 3$.

Combining these, the spectral bound (28) for a single context gives

$$D(G_\alpha, \hat{\rho}) \leqslant \kappa\sqrt{1 - E} \approx 7.35 \times 0.561 \approx 4.12. \tag{55}$$

The commutator of the outer observables in the context G_α (52) can be computed directly. Since $[\hat{A}_{\mathbf{k}}, \hat{A}_{\mathbf{k}'}] = 4[\hat{P}_{0_{\mathbf{k}}}, \hat{P}_{0_{\mathbf{k}'}}]$, where $\hat{P}_{0_{\mathbf{k}}} = |0_{\mathbf{k}}\rangle\langle 0_{\mathbf{k}}|$, it is sufficient to evaluate the projector commutator. For rank-1 projectors $\hat{P}$ and $\hat{Q}$ with overlap $|\langle 0_{\mathbf{k}}|0_{\mathbf{k}'}\rangle|^2 = \cos^2\gamma$, one has $\|[\hat{P}, \hat{Q}]\|_{\mathrm{op}} = \cos\gamma\sin\gamma$, and therefore

$$\left\| \left[\hat{A}_{\alpha-1}, \hat{A}_{\alpha+1}\right] \right\|_{\mathrm{op}} = 4\sqrt{\sqrt{5} - 2} \approx 1.94. \tag{56}$$

This operator-norm bound is substantially tighter than the spectral bound, differing by a factor exceeding two.

For pure states ($\beta = 1$), the hybrid bound (36) therefore reduces to the operator-norm bound for all KCBS contexts. Summing over all five contexts yields the global bound

$$D(G, \hat{\rho}) \leqslant 5 \times 1.94 \approx 9.72. \tag{57}$$

5.3. Geometric visualization via the Majorana-stellar representation

The Majorana-stellar representation [35] provides a geometric framework for visualizing spin-s states as constellations on the Bloch–Poincaré sphere. Beyond visualization, this representation offers significant computational advantages: inner products, expectation values and projector overlaps reduce to elementary functions of angles between stellar directions, bypassing explicit matrix algebra. This geometric formalism has also been used in detailed analyses of spin-1 state geometry, notably in the work of Aravind [36]. The Majorana-stellar representation thus furnishes a common geometric platform on which both the operational contextuality measure $D(G, \hat{\rho})$ and the uncertainty products $(\Delta A)(\Delta C)$ can be analyzed and visualized. For spin-1, the three basis states $|+1_{\mathbf{k}}\rangle$, $|0_{\mathbf{k}}\rangle$, $|-1_{\mathbf{k}}\rangle$ are each represented by a pair of Majorana stars, and any pure state is a superposition of these basis vectors. The eigenstates of $\hat{S}_{\mathbf{k}}$ take the forms

$$|+1_{\mathbf{k}}\rangle \equiv |+k+k\rangle, \quad |0_{\mathbf{k}}\rangle \equiv \tfrac{1}{\sqrt{2}}\left(|+k-k\rangle + |-k+k\rangle\right), \quad |-1_{\mathbf{k}}\rangle \equiv |-k-k\rangle, \tag{58}$$

where the notation $|\pm k\rangle$ denotes spin-$\frac{1}{2}$ states along direction $\pm\mathbf{k}$. The $m_s = 0$ state thus corresponds to two antipodal stars aligned with $\mathbf{k}$, while the $m_s = \pm 1$ states correspond to coincident stars. These Majorana-stellar representations of the spin-1 eigenstates are illustrated in figure 2.

A general pure spin-1 state with Majorana directions $\mathbf{m}$ and $\mathbf{n}$ can be written as

$$|\chi\rangle = \frac{1}{\sqrt{3 + \mathbf{m}\cdot\mathbf{n}}}\left(|+m+n\rangle + |+n+m\rangle\right), \tag{59}$$

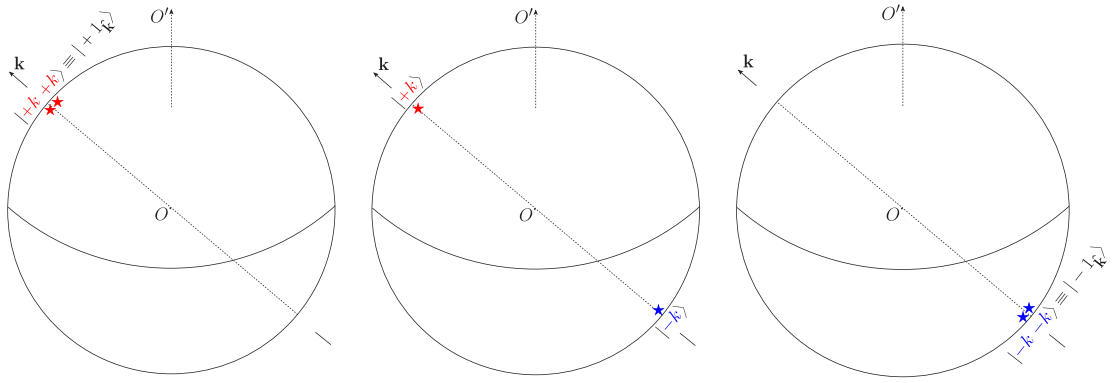

(a) $|+1_{\mathbf{k}}\rangle \equiv |+k\,+k\rangle$. (b) $|0_{\mathbf{k}}\rangle \equiv \frac{1}{\sqrt{2}}(|+k-k\rangle + |-k+k\rangle)$. (c) $|-1_{\mathbf{k}}\rangle \equiv |-k\,-k\rangle$.

Figure 2. Majorana-stellar representations of a spin-1 system's eigenstates along a direction **k**.

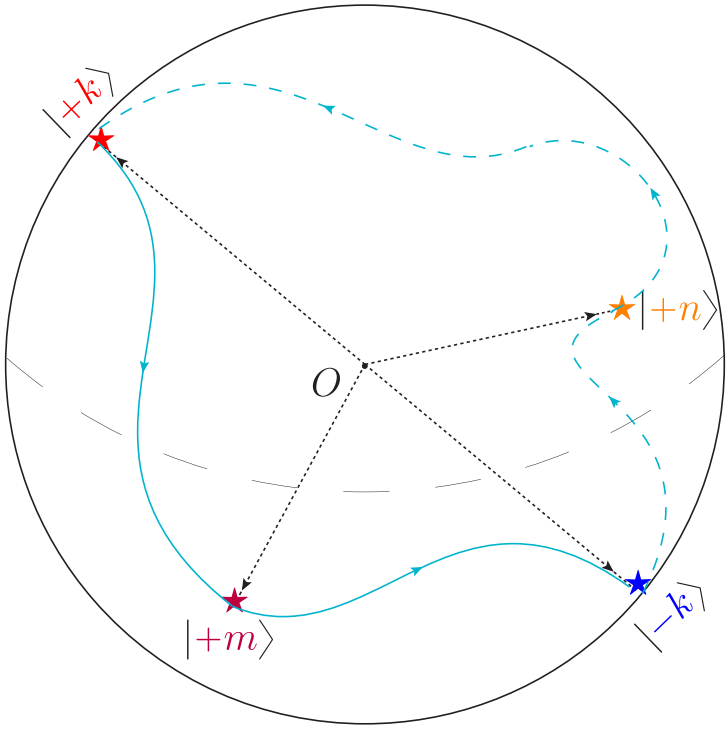

Figure 3. A spin-1 state in the Majorana-stellar representation: $|\chi\rangle = \frac{1}{\sqrt{3+\mathbf{m}\cdot\mathbf{n}}}\left(|+m+n\rangle + |+n+m\rangle\right)$. Its projection onto the $m_s = 0$ eigenstate along direction **k** is visualized as a trajectory on the BP sphere.

and its overlap with the $m_s = 0$ state along **k** determines the expectation value $\langle\chi|\hat{P}_{0_{\mathbf{k}}}|\chi\rangle$. Its representation in the Majorana-stellar formalism, together with the corresponding projection onto the $m_s = 0$ eigenstate, is illustrated in figure 3.

The uncertainty of the dichotomic observable $A_{\mathbf{k}}$ in state $|\chi\rangle$ is

$$(\Delta A_{\mathbf{k}})^2 = 4p_{\mathbf{k}}(1-p_{\mathbf{k}}), \qquad p_{\mathbf{k}} = \langle\chi|\hat{P}_{0_{\mathbf{k}}}|\chi\rangle, \tag{60}$$

and is maximized when $p_{\mathbf{k}} = \frac{1}{2}$. The geometric interpretation of maximum-uncertainty states in the Majorana-stellar representation is summarized in figure 4. For spin-1, the MSR yields a three-dimensional Euclidean-like visualization of the Hilbert space. Within this geometric picture, the maximum-uncertainty condition defines a plane perpendicular to **k**, spanned by the directions of the other two observables in the same context (see figure 4). States that exhibit maximum uncertainty for $A_{\mathbf{k}}$ have a Majorana constellation lying on this plane.

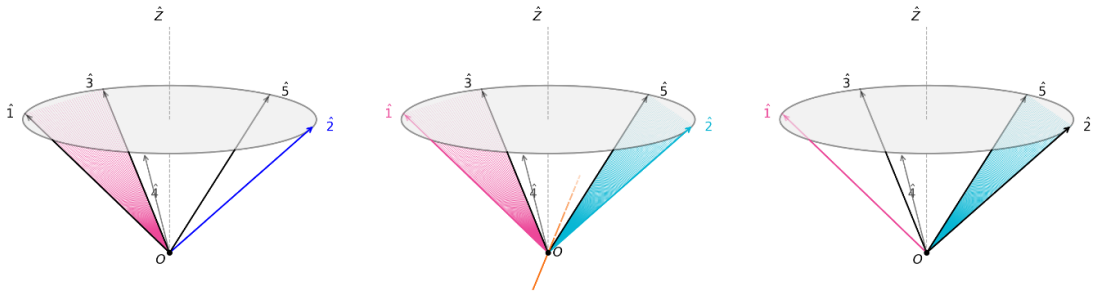

(a) The pink surface, perpendicular to the axis $\hat{\mathbf{2}}$, is spanned by axes $\hat{\mathbf{1}}$ and $\hat{\mathbf{3}}$.

(b) States represented on the intersection line of the pink and blue surfaces, shown here by orange line, exhibit maximum uncertainty for both $A_{\mathbf{1}}$ and $A_{\mathbf{2}}$.

(c) The blue surface, perpendicular to the axis $\hat{\mathbf{1}}$, is spanned by axes $\hat{\mathbf{2}}$ and $\hat{\mathbf{5}}$.

Figure 4. Maximum uncertainty for an observable $A_{\mathbf{k}}$ of a spin-1 system occurs for the states that can be represented on the surface perpendicular to direction $\mathbf{k}$ in the Majorana-stellar representation. This surface is the one spanned by the directions along which the other two observables of the same context are defined. Two such surfaces and their intersection are shown. All the 5 directions $\hat{\mathbf{1}} - \hat{\mathbf{5}}$ correspond to those in the KCBS pentagram of figure 1(a).

For two different directions $\mathbf{k}$ and $\mathbf{k'}$, the associated maximum-uncertainty planes intersect along a curve (as shown in figure 4(b)). However, for three or more contexts, the corresponding planes do not generically share a common line; hence true maximum uncertainty cannot be achieved simultaneously for all contexts. Instead, one seeks the state that optimizes the sum of uncertainty products. For the full KCBS family of five contexts, this optimization yields a unique state: $|0_{\mathbf{z}}\rangle$, the $m_s = 0$ eigenstate along the symmetry axis (see figure 5). A detailed classification of the maximum-uncertainty sets for one to five KCBS contexts, together with the corresponding optimal uncertainty sums, is provided in table 1 of the Supplementary Information.

Further geometric characterizations of spin-1 states in terms of orthonormal triads, including explicit coefficient formulas for the decomposition $|\chi\rangle = K|\hat{K}\rangle + K_1|\hat{K}_1\rangle + K_2|\hat{K}_2\rangle$, are developed in SI, section D.

5.4. States achieving extremal uncertainty products

The KCBS pentagram and the unique maximum-uncertainty state $|0_{\mathbf{z}}\rangle$ are shown in figure 5. The state $|0_{\mathbf{z}}\rangle$ achieves the optimal sum of uncertainty products

$$\sum_{\alpha=1}^{5} (\Delta A_{\alpha-1})\,(\Delta A_{\alpha+1}) = 4\left(\sqrt{5}-1\right) \approx 4.94, \tag{61}$$

with each context contributing equally: $(\Delta A_{\alpha-1})(\Delta A_{\alpha+1}) = \frac{4(\sqrt{5}-1)}{5} \approx 0.99$ per context. The state $|0_{\mathbf{z}}\rangle$ is identified as the maximizer of the left-hand side of equation (61) by numerical optimization over all pure spin-1 states—a result consistent with the geometric analysis of section 5.3, where the intersection of all five maximum-uncertainty planes singles out the symmetry axis (see also SI, section D.6 and table 1). The value $4(\sqrt{5}-1)$ is then verified by direct calculation: since $(\Delta A_{\mathbf{k}})^2 = 4p_{\mathbf{k}}(1-p_{\mathbf{k}})$ with $p_{\mathbf{k}} = |\langle 0_{\mathbf{k}}|\chi\rangle|^2$ (see SI, section D.4), and the pentagonal symmetry yields $p_{\mathbf{k}} = |\langle 0_{\mathbf{k}}|0_{\mathbf{z}}\rangle|^2 = \frac{1}{\sqrt{5}}$ for all five directions, each uncertainty product equals $4p(1-p) = \frac{4(\sqrt{5}-1)}{5}$, and summing the five identical contributions yields equation (61).

A remarkable feature of this maximizing state—and more generally of all states of the form $|0_{\hat{\mathbf{u}}}\rangle$ for any axis $\hat{\mathbf{u}}$—is that the operational contextuality measure vanishes:

$$D(G, |0_{\hat{\mathbf{u}}}\rangle\langle 0_{\hat{\mathbf{u}}}|) = \sum_{\alpha=1}^{5} \left|\langle 0_{\hat{\mathbf{u}}}| \left[\hat{A}_{\alpha-1}, \hat{A}_{\alpha+1}\right] |0_{\hat{\mathbf{u}}}\rangle\right| = 0. \tag{62}$$

To see why, note that $\hat{A}_{\mathbf{k}} = 2(\hat{\mathbf{S}}\cdot\mathbf{k})^2 - \hat{I}$ is a rank-2 quadrupolar (spin-tensor) operator, even under time reversal: $\hat{\Theta}\hat{A}_{\mathbf{k}}\hat{\Theta}^{-1} = \hat{A}_{\mathbf{k}}$. States of the form $|0_{\hat{\mathbf{u}}}\rangle$ are time-reversal invariant, $\hat{\Theta}|0_{\hat{\mathbf{u}}}\rangle = |0_{\hat{\mathbf{u}}}\rangle$. The commutator $[\hat{A}_{\alpha-1}, \hat{A}_{\alpha+1}]$ is anti-Hermitian, so its expectation value is purely imaginary. At the same time,

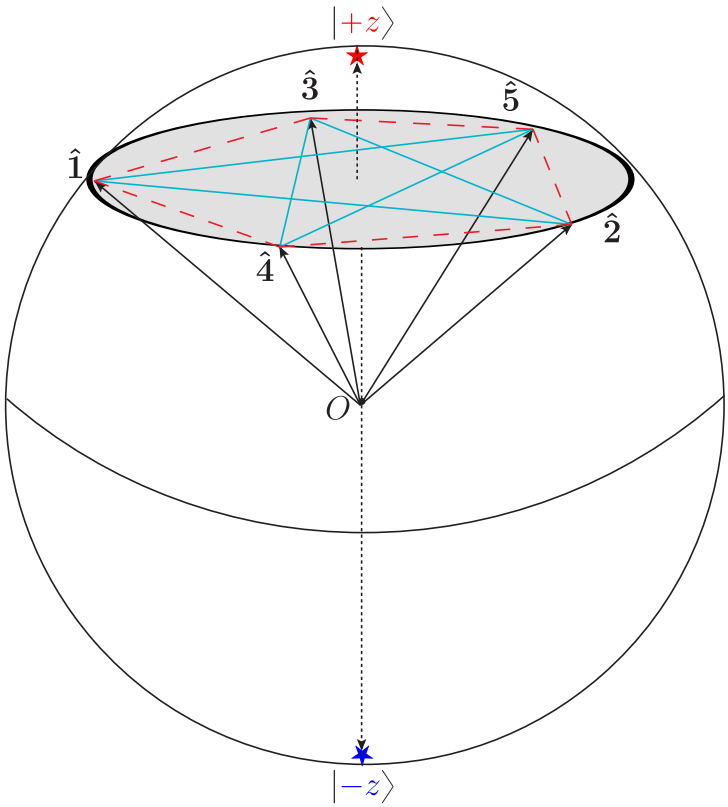

Figure 5. KCBS pentagram and the state $|0_{\mathbf{z}}\rangle$ represented by a Majorana constellation composed of two stars, located on the BP sphere; $|0_{\mathbf{z}}\rangle = \frac{1}{\sqrt{2}}(|+z-z\rangle + |-z+z\rangle) \equiv |\hat{Z}\rangle$.

because both operators are time-reversal even, the commutator itself is also time-reversal even, and its expectation value in a time-reversal-invariant state must be real. Being simultaneously real and purely imaginary, each expectation value $\langle 0_{\hat{\mathbf{u}}}|[\hat{A}_{\alpha-1}, \hat{A}_{\alpha+1}]|0_{\hat{\mathbf{u}}}\rangle$ vanishes identically, yielding $D = 0$. The key contrast is thus between the *symmetric* (variance-based) uncertainty products, which are maximized by the high–symmetry state $|0_{\mathbf{z}}\rangle$, and the *antisymmetric* commutator expectation that defines the operational contextuality, which vanishes for the same state.

Consequently, the Robertson lower bound (44) becomes trivial for these states:

$$\frac{1}{2}D(G, |0_{\hat{\mathbf{u}}}\rangle\langle 0_{\hat{\mathbf{u}}}|) = 0 \leqslant \sum_{\alpha} (\Delta A_{\alpha-1})(\Delta A_{\alpha+1}). \tag{63}$$

The bound is satisfied but provides no constraint on the uncertainty products. This illustrates that maximum uncertainty and maximum operational contextuality are achieved by *different* quantum states in the KCBS scenario.

In contrast, generic states such as $|\pm 1_{\mathbf{z}}\rangle$ exhibit nonzero operational contextuality. For these eigenstates of $\hat{S}_{\mathbf{z}}$, numerical evaluation gives $D(G, |\pm 1_{\mathbf{z}}\rangle\langle \pm 1_{\mathbf{z}}|) \approx 6.50$, which represents approximately 67% of the global operator-norm bound $5 \times 1.94 \approx 9.72$. The Robertson lower bound then yields $\frac{1}{2}D \approx 3.25$, while the actual uncertainty product is $\sum_{\alpha}(\Delta A_{\alpha-1})(\Delta A_{\alpha+1}) = 4.00$, leaving a gap of approximately 0.75.

5.5. Summary of the KCBS analysis

The KCBS scenario provides a concrete illustration of the full framework. The MIE $E \approx 0.685$ quantifies the intrinsic contextuality of each pentagonal context, while the operator-norm bound $\|[\hat{A}, \hat{C}]\|_{\text{op}} \approx 1.94$ provides the tightest constraint on the operational measure $D(G_{\alpha}, \hat{\rho})$—substantially sharper than the spectral bound of 4.12 per context.

The Majorana-stellar representation reveals that the state achieving the optimal sum of uncertainty products is unique: $|0_{\mathbf{z}}\rangle$, which attains $\sum_{\alpha}(\Delta A_{\alpha-1})(\Delta A_{\alpha+1}) = 4(\sqrt{5}-1) \approx 4.94$ yet has vanishing

operational contextuality $D = 0$. This decoupling between uncertainty products and commutator expectations demonstrates that the Robertson inequality, while always valid, can become uninformative precisely in regimes of greatest physical interest, where uncertainty is extremal and operational signatures are expected to be most pronounced.

The hierarchy of bounds developed in sections 3 and 4 is thus fully verified in the KCBS setting, with the operator-norm bound emerging as the relevant constraint for this geometry.

6. Conclusion

Contextuality lies at the heart of quantum theory [37–39], and constitutes a key resource for quantum information processing and computation [40–49]. It unifies several of the most striking features of quantum mechanics, including the incompatibility of measurements [2, 16], entanglement [50–52] and nonlocality [53–56]. A complete understanding and systematic quantification of contextuality is therefore essential, both for foundational reasons and for practical applications in quantum technologies.

In this work we have proposed an information-theoretic framework for quantifying Kochen–Specker contextuality. Two complementary measures were introduced: the MIE $E(B;A,C)$, a state-independent quantity that captures the geometric overlap between the joint eigenspaces of $(\hat{A},\hat{B})$ and $(\hat{C},\hat{B})$ within each context, thereby characterizing the incompatibility between A and C; and the operational measure $D(G,\hat{\rho})$, a state-dependent quantity that reflects the contextual behavior of observables through commutator expectation values. The MIE, inspired by Onicescu's information energy, equals unity for noncontextual configurations, and decreases as contextuality increases. The operational measure provides an experimentally accessible signature, directly tied to the Robertson uncertainty relation.

We established a hierarchy of bounds connecting these measures to the uncertainty products of incompatible observables. The spectral bound relates D to the MIE through the prefactor $\kappa = \sqrt{2d}(\sum_i a_i^2)^{1/2}(\sum_j c_j^2)^{1/2}$, while a purity correction tightens this bound for mixed states. More significantly, the operator-norm bound $D \leqslant \|[\hat{A},\hat{C}]\|_{\mathrm{op}}$, can provide a tighter constraint than the spectral estimate, as demonstrated explicitly for the KCBS scenario. The hybrid bound, taking the minimum of spectral and operator-norm estimates, provides the most refined upper limit available from these methods.

Application to the KCBS scenario—the minimal contextuality configuration in a three-dimensional Hilbert space—yielded explicit closed-form expressions for all quantities. The pentagonal geometry fixes the MIE at $E \approx 0.685$ for each context, with the operator-norm bound (≈ 1.94 per context) being more than twice as tight as the corresponding spectral bound (≈ 4.12 per context). The Majorana-stellar representation provided both computational advantages and geometric insight: for spin-1, it yields a three-dimensional Euclidean-like visualization in which maximum-uncertainty states for a given observable lie on the plane perpendicular to that observable's direction. Since three or more maximum-uncertainty planes cannot share a common intersection, simultaneous maximum uncertainty is unattainable; the state $|0_{\mathbf{z}}\rangle$ instead optimizes the sum of uncertainty products, achieving the global maximum $\sum_\alpha (\Delta A_{\alpha-1})(\Delta A_{\alpha+1}) = 4(\sqrt{5}-1)$.

A notable finding concerns the relationship between operational contextuality and uncertainty. States of the form $|0_{\hat{\mathbf{u}}}\rangle$—which achieve the optimal sum of uncertainty products—exhibit vanishing operational contextuality ($D = 0$) due to the quadrupolar symmetry of the KCBS observables. For these states the Robertson inequality becomes trivial, providing no constraint on the uncertainties. In contrast, generic states such as $|\pm 1_{\mathbf{z}}\rangle$ display substantial operational contextuality ($D \approx 6.50$) with a nontrivial Robertson lower bound. This demonstrates that maximum uncertainty and maximum operational contextuality are achieved by distinct quantum states, revealing a subtle interplay between these fundamental aspects of quantum mechanics. Whether this decoupling persists in other contextuality scenarios—where the quadrupolar observable structure and rotational symmetry specific to KCBS may not hold—warrants systematic investigation.

The geometric approach developed here, combining the MIE with the Majorana-stellar visualization, offers a unified and operationally transparent perspective on contextuality in finite-dimensional quantum systems. Extensions to higher-dimensional quantum systems and alternative contextuality scenarios, as well as experimental implementations of the operational measure, represent promising directions for future investigation.

Acknowledgements

Part of this work was carried out at Bilimler Köyü, Foça, Türkiye. The authors thank Erbuğ Kaya for assistance with the figures.

Data availability statement

All data that support the findings of this study are included within the article (and any supplementary files). The Python verification codes used for the numerical computations are available at https://sites.google.com/mersin.edu.tr/nicem-duzenegi/english.

Supplementary Information available at https://doi.org/10.1088/1751-8121/ae67c0/data1.

Conflict of interest

The authors declare that there are no conflicts of interest regarding the publication of this article

Ethics statement

This study does not involve human participants, animals, or any identifiable personal data, and therefore did not require ethical approval.

Funding statement

This research received no external funding.

Author contributions (CRediT)

A.C.G.: Conceptualization, Methodology, Formal analysis, Investigation, Writing—original draft, Writing—review & editing, Visualization. Z.G.: Conceptualization, Supervision, Writing—review & editing.

ORCID iDs

A C Günhan 0000-0003-0050-2484
Z Gedik 0000-0001-6928-6156

References

[1] Nielsen M A and Chuang I L 2010 *Quantum Computation and Quantum Information: 10th Anniversary edn* (Cambridge University Press)
[2] Bell J S 1966 On the problem of hidden variables in quantum mechanics *Rev. Mod. Phys.* **38** 447–52
[3] Zeilinger A 2005 The message of the quantum *Nature* **438** 743 Most physicists view the experimental confirmation of the quantum predictions as evidence for nonlocality. But I think that the concept of reality itself is at stake, a view that is supported by the Kochen–Specker paradox..
[4] Hermann G 1935 Die naturphilosophischen grundlagen der quantenmechanik *Abhandlungen der Fries'schen Schule* **6** 75–152
[5] Hermann G 1935 Die naturphilosophischen grundlagen der quantenmechanik *Naturwissenschaften* **23** 718–21
Lumma D 1999 *Harvard Rev. Phil.* **7** 35–44 Translated into English with a brief introduction
[6] Peres A 1990 Incompatible results of quantum measurements *Phys. Lett. A* **151** 107–8
[7] Gleason A M 1957 Measures on the Closed Subspaces of a Hilbert Space *J. Math. Mech.* **6** 885–93
[8] Specker E 1960 Die logik nicht gleichzeitig entscheidbarer Aussagen *Dialectica* **14** 239–46
[9] Kochen S B and Specker E P 1967 The problem of hidden variables in quantum mechanics *J. Math. Mech.* **17** 59–87
[10] Redhead M 1987 *Incompleteness, Nonlocality and Realism: A Prolegomenon to the Philosophy of Quantum Mechanics* (Oxford University Press)
[11] Peres A 1991 Two simple proofs of the Kochen-Specker theorem *J. Phys. A: Math. Gen.* **24** L175
[12] Budroni C, Cabello A, Gühne O, Kleinmann M and Larsson J-A 2022 Kochen-specker contextuality *Rev. Mod. Phys.* **94** 045007
[13] Svozil K 2012 How much contextuality? *Nat. Comput.* **11** 2621–265

[14] Kleinmann M, Gühne O, Portillo J R, Larsson J-A and Cabello A 2011 Memory cost of quantum contextuality *New J. Phys.* **13** 113011
[15] Brunner N, Cavalcanti D, Salles A and Skrzypczyk P 2011 Bound nonlocality and activation *Phys. Rev. Lett.* **106** 020402
[16] Popescu S and Rohrlich D 1994 Quantum nonlocality as an axiom *Found. Phys.* **24** 379–85
[17] van Dam W, Gill R D and Grünwald P D 2005 The statistical strength of nonlocality proofs *IEEE Trans. Inf. Theory* **51** 2812–35
[18] Grudka A, Horodecki K, Horodecki M, Horodecki P, Horodecki R, Joshi P, Kłobus W and Wójcik A 2014 Quantifying Contextuality *Phys. Rev. Lett.* **112**
[19] Abramsky S, Barbosa R S and Mansfield S 2017 Contextual fraction as a measure of contextuality *Phys. Rev. Lett.* **119** 050504
[20] Kujala J V and Dzhafarov E N 2019 Measures of contextuality and non-contextuality *Phil. Trans. R. Soc. A* **377** 20190149
[21] Pitowsky I 1991 Correlation polytopes: their geometry and complexity *Math. Program.* **50** 395–414
[22] Kleinmann M, Budroni C, Larsson J-A, Gühne O and Cabello A 2012 Optimal inequalities for state-independent contextuality *Phys. Rev. Lett.* **109** 250402
[23] Shannon C and Weaver W 1949 The mathematical theory of communication *No. 1. c. in Illini Books* (University of Illinois Press)
[24] Rényi A 1961 On measures of information and entropy *Proc. 4th Berkeley Symp. on Mathematical Statistics and Probability, 1960* vol 4 (University of California Press) pp 547–61
[25] Onicescu O 1966 Theorie de l'information energie informationelle *Comptes Rendus de l'Academie Des Sci. Series AB* **263** 841–2
[26] Björck Å and Golub G H 1973 Numerical methods for computing angles between linear subspaces *Math. Comp.* **27** 579–94
[27] Ivonovic I 1981 Geometrical description of quantal state determination *J. Phys. A: Math. Gen.* **14** 3241–5
[28] Wootters W K and Fields B D 1989 Optimal state-determination by mutually unbiased measurements *Ann. Phys.* **191** 363–81
[29] Bengtsson I, Blanchfield K and Cabello A 2012 A Kochen–Specker inequality from a SIC *Phys. Lett. A* **376** 374–6
[30] Busch P, Lahti P J and Mittelstaedt P 1996 The quantum theory of measurement *Lecture Notes in Physics Monographs* vol m2, 2nd edn (Springer)
[31] Peres A 2002 *Quantum Theory: Concepts And Methods* (Kluwer Academic Publishers)
[32] Klyachko A A, Can M A, Binicioğlu S and Shumovsky A S 2008 Simple test for hidden variables in spin-1 systems *Phys. Rev. Lett.* **101** 020403
[33] Cabello A 2014 Exclusivity principle and the quantum bound of the Bell inequality *Phys. Rev. A* **90** 062125
[34] Robertson H P 1929 The uncertainty principle *Phys. Rev.* **34** 163–4
[35] Majorana E 1932 Atomi orientati in campo magnetico variabile *Il Nuovo Cimento (1924-1942)* **9** 43–50
[36] Aravind P 2017 MUBs and SIC-POVMs of a spin-1 system from the majorana approach (arXiv:1707.02601[quant-ph])
[37] Heisenberg W 1925 Über quantentheoretische umdeutung kinematischer und mechanischer beziehungen *Z. Phys.* **33** 879–93
[38] The Nobel Foundation The nobel prize in physics 1932 was awarded to Werner Karl Heisenberg '*for the creation of quantum mechanics*, the application of which has, inter alia, led to the discovery of the allotropic forms of hydrogen (available at: https://www.nobelprize.org/prizes/physics/1932/summary/)
[39] Sakurai J J and Napolitano J 2017 *Modern Quantum Mechanics* 2nd edn (Cambridge University Press)
[40] Heywood P and Redhead M L G 1983 Nonlocality and the Kochen-Specker paradox *Found. Phys.* **13** 481–99
[41] Bechmann-Pasquinucci H and Peres A 2000 Quantum cryptography with 3-state systems *Phys. Rev. Lett.* **85** 3313–6
[42] Spekkens R W 2008 Negativity and contextuality are equivalent notions of nonclassicality *Phys. Rev. Lett.* **101** 020401
[43] Aharon N and Vaidman L 2008 Quantum advantages in classically defined tasks *Phys. Rev. A* **77** 052310
[44] Svozil K 2009 Three criteria for quantum random-number generators based on beam splitters *Phys. Rev. A* **79** 054306
[45] Cabello A 2010 Proposal for revealing quantum nonlocality via local contextuality *Phys. Rev. Lett.* **104** 220401
[46] Waegell M and Aravind P 2013 GHZ paradoxes based on an even number of qubits *Phys. Lett. A* **377** 546–9
[47] Abramsky S, Barbosa R S, Kishida K, Lal R and Mansfield S 2025 Contextuality, cohomology and paradox *24th EACSL Annual Conf. on Computer Science Logic (CSL 2015)* (*Leibniz Int. Proc. in Informatics (LIPIcs)*) (*Germany*) vol 41, ed S Kreutzer (Dagstuhl) Schloss Dagstuhl–Leibniz-Zentrum fuer Informatik 2015 pp 211–28
[48] Raussendorf R 2013 Contextuality in measurement-based quantum computation *Phys. Rev. A* **88** 022322
[49] Frembs M, Roberts S and Bartlett S D 2018 Contextuality as a resource for measurement-based quantum computation beyond qubits *New J. Phys.* **20** 103011
[50] Schrödinger E 1935 Die gegenwärtige situation in der quantenmechanik *Naturwissenschaften* **23** 807–12
[51] Einstein A, Podolsky B and Rosen N 1935 Can quantum-mechanical description of physical reality be considered complete? *Phys. Rev.* **47** 777–80
[52] Bohm D 1951 *Quantum Theory* 1st edn (Prentice-Hall)
[53] Bell J S 1964 On the einstein podolsky rosen paradox *Phys. Phys. Fiz.* **1** 195–200
[54] Stapp H P 1975 Bell's theorem and world process *Il Nuovo Cimento B (1971–1996)* **29** 270–6
[55] Bell J S and Aspect A 2004 *Speakable and Unspeakable in Quantum Mechanics: Collected Papers on Quantum Philosophy* 2nd edn (Cambridge University Press)
[56] Gisin N 1996 Hidden quantum nonlocality revealed by local filters *Phys. Lett. A* **210** 151–6